Differential leaf-to-root movement, trophic transfer, and tissue-specific biodistribution of metal-based and polymer-based nanoparticles when present singly and in mixture

Chen, Y.; He, E.; Peijnenburg, W.J.G.M.; Jiang, X.; Qiu, H.

Environmental Science & Technology

pubs.acs.org/est

Article

Differential Leaf-to-Root Movement, Trophic Transfer, and Tissue-Specific Biodistribution of Metal-Based and Polymer-Based Nanoparticles When Present Singly and in Mixture

Yingxin Chen, Erkai He, Willie J.G.M. Peijnenburg, Xiaofeng Jiang, and Hao Qiu*

Cite This: *Environ. Sci. Technol.* 2024, 58, 21025−21036

Read Online

ACCESS | Metrics & More | Article Recommendations | Supporting Information

ABSTRACT: The transfer of nanoparticles (NPs) through the terrestrial food chain via foliar uptake presents poorly understood risks, especially in scenarios involving copollution and plant translocation. Herein, we exposed the radishes to single and mixed foliar doses of CeO_2 NPs and deuterated polystyrene (DPS), investigating the trophic transfer of NPs from radish shoots/roots to snails. Compared to single treatments, mixture treatments increased Ce uptake by plants but had no effect on DPS uptake. Additionally, mixture treatments did not affect the movement of Ce and DPS from shoots to roots. Under NP mixture exposure, trophic transfer efficiencies (TTF) for Ce (2.09×10^{-2}) and DPS (2.54×10^{-2}) significantly decreased in shoot-feeding snails. In root-feeding snails, TTF for Ce (3.32×10^{-1}) also showed a significant decrease, while TTF for DPS remained unchanged. Mixture treatments exhibited differential impacts on different snail body parts, particularly leading to biomagnification of DPS in the digestive glands and soft tissues (TTF > 1) of snails consuming roots exposed to mixtures. Both CeO_2 and DPS displayed a sudden increase in assimilation efficiency following translocation to the roots. This study provides insights into changes during trophic transfer due to coexposure and plant translocation processes associated with nanoparticles, enhancing our comprehension regarding their environmental risks.

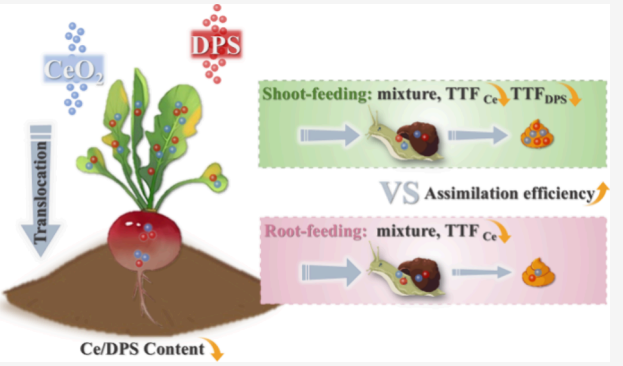

KEYWORDS: *food chain, CeO_2 nanoparticles, deuterated polystyrene, foliar exposure, trophic transfer*

INTRODUCTION

Nanoparticles (NPs) refer to materials with at least one dimension measuring below 100 nm. Metal-based engineered nanomaterials (ENMs) and polymer-based nanoplastics are two well-known types of functional materials within this category.[1] Engineered nanomaterials are intentionally manufactured materials designed for specific applications, typically with uniform compositions, while nanoplastics mainly result from the decomposition of plastic waste in the environment.[2,3] The development of new industrial materials has led to their widespread presence in societally relevant products and the environment. Plastic production has dramatically increased over time, from 1.5 million tons in 1950 to 390 million tons in 2021.[4] Global ENMs production is estimated to range from several thousand to no more than one million tons annually.[5] However, our understanding of the environmental risks associated with nanomaterials lags behind our ability to design and apply these materials. This has resulted in concerns about "nano-pollution" on a global scale.[6,7] Numerous studies have been conducted in soil and water environments, revealing the potential adverse effects of NPs exposure on organisms and their subsequent transfer through the food chain.[8,9] While it is known that NPs can exist as fine particulates in the atmosphere for extended periods, there is a lack of research on their regional and global exposure pathways.[10] Plants act as a natural "green barrier" on the earth's surface, with their leaves serving as the primary sites for atmospheric NPs deposition and accumulation. After being deposited onto the leaf surface, NPs are primarily taken up by leaves through stomata, hydathodes, and cuticle permeability.[11−14] The uptake of NPs is influenced by key factors such as size, surface area, chemical composition, and hydrophilicity/hydrophobicity.[15,16] The size exclusion limit for NP uptake varies among plant species due to physiological and anatomical differences but generally falls below 100 nm.[17−20] In real-world scenarios, NPs may undergo aggregation, dissolution, transformation, and deposition under biological or abiotic pressures, which can significantly impact their characteristics. Unlike extensive research on NP transfer

Received: June 17, 2024
Revised: November 3, 2024
Accepted: November 5, 2024
Published: November 12, 2024

through the root system, limited studies have focused on exploring and examining how these particles are taken up by plant leaves from the atmosphere and subsequently transferred through the food chain to higher trophic levels. Given the crucial ecological role of food-source plants as primary producers and their function as important pathways for pollutants entering herbivores and human bodies, it is imperative that further research be conducted on the exposure of leaf surfaces to NPs in the food chain.

Previous research has demonstrated that various types of NPs can be taken up by plants and be transferred along the food chain, including TiO_2, Ag_2O, CeO_2, Fe_3O_4, and ZnO NPs.[21−26] For instance, in the tobacco−tobacco hornworm (*Nicotiana tabacum-Manduca sexta*) food chain, plants took up 5, 10, and 15 nm gold NPs through hydroponics, which resulted in bioaccumulation factors of 6.2, 11.6, and 9.6, respectively.[27] However, studies have also shown uptake and internalization by plants but no significant accumulation and biomagnification of, for instance, CeO_2 NPs in the lettuce-hornworm-chicken (*Lactuca sativa - Spodoptera litura - Gallus gallus domesticus*) and pakchoi-snail (*Brassica chinensis - Achatina fulica*) food chains.[22,28] These studies primarily focus on describing differences in transfer efficiency caused by morphological and size variations within a single material due to high variability between different NPs flows across trophic levels. However, when considering the coexistence of nanomaterials such as representative ENMs and nanoplastics present in mixtures, their transport within the food chain remains largely unknown due to several reasons. First, there are significant differences in chemical composition and density between metal-based and polymer-based NPs, which makes it challenging to extrapolate data from single exposures alone.[29] Moreover, the coexistence of NPs may lead to interaction that result in the formation of complex pollutants, thereby altering the environmental behavior of individual NPs and subsequently affecting plant accumulation and food chain transfer. Additionally, the mechanisms for nanoplastics transfer within the food chain remain unknown due to limitations associated with detecting carbon-based materials in organisms amidst the typical carbon-rich context of biota.

Additionally, nanoparticles can relocate to other plant organs following internalization and several studies have documented the biotransformation of certain NPs (such as CuO, CeO_2, and Se NPs) in different parts of plants like rice and cucumber.[23,30−32] It is reasonable to hypothesize that leaf-exposed NPs may migrate toward the roots, thereby influencing NP transfer efficiency along food chains and their bioavailability. To our knowledge, no investigations have been conducted to compare the performance of NPs stored in various plant organs, particularly edible parts, with respect to trophic transfer along the food chain and their subsequent impact on consumers. This comparison is crucial considering the stochastic feeding behavior of animals consuming different plant components. Cherry radish (*Raphanus sativus* L.) is an important cruciferous food crop with edible parts ranging from above-ground green leaves to swollen underground taproot.[33] CeO_2 is among one of globally most-produced ENMs and is widely used in industrial applications like polishing agents, catalysts, preservatives, and sensors.[34] In agriculture specifically, it serves as growth regulator, pesticide, fertilizer, nutrient, or drug carrier.[35] Moreover, field studies have demonstrated the presence of polystyrene (PS) micro- and nanoplastics on plant surfaces.[36−39] Additionally, CeO_2 NPs are utilized as additives to enhance the mechanical strength and thermal stability of PS products.[40,41] Based on realistic scenarios, representative NPs chosen were CeO_2 and PS, capable of reaching plants either through intentional artificial application or nonspontaneous atmospheric deposition leading to foliar coexposure.

In this study, we have established a food chain involving cherry radish (shoot/root) and snails. For the first time, we synthesized deuterated polystyrene (DPS) in order to address the challenges of detecting carbon-based materials within the carbon-rich context of organisms. Our hypothesis is 2-fold: 1) Foliar exposure to a mixture of NPs affects the uptake and translocation of CeO_2/DPS in plants as compared to exposure to the individual particles, 2) Nanoparticles stored in leaves and roots behave differently regarding trophic transfer efficiency and consumer accumulation as well as distribution under single and mixed exposure modes. The results of this study will enhance our understanding of how DPS-CeO_2 mixtures behave in organisms through the food chain pathway.

MATERIALS AND METHODS

Preparation of NPs and Organism. Following the method described by Tian et al., with minor modifications, deuterium-labeled styrene monomers were used to synthesize DPS NPs via emulsion polymerization (Text S1).[42] The chemical structure of the synthesized DPS was confirmed using μ-Fourier transform infrared (μ-FTIR) (Nicolet iN10, Thermo Fisher Scientific, USA) (Figure S1), with a deuterium substitution rate of the target product reaching 85%. The CeO_2 NPs, with a purity >99.95% and a particle size <50 nm, were procured from Sigma-Aldrich (St. Louis, Missouri, USA).

The morphology, particle size, and zeta potential of the two types of nanomaterials were characterized using transmission electron microscopy (TEM) (Tecani G2 Spirit TWIN, FEI, Netherlands) and dynamic light scattering (DLS) (Anton Paar Litesizer 500, Graz, Austria), as outlined in Table 1.

Table 1. Material Characterization Parameters of Nanoparticle (NP) Solutions from Different Treatment Groups at a Concentration of 100 mg/L, Including CeO_2, DPS, and Their Mixtures

Parameters	CeO_2	DPS	Mixture
pH	5.90	5.96	5.91
Polydispersity index	0.264	0.238	0.231
Zeta potential (mV)	−28.4 ± 1.3[aa]	−26.4 ± 1.2[a]	−28.6 ± 1.1[a]
Average particle size	47.8 ± 10.8	80.7 ± 0.8	/
Hydrodynamic size	417 ± 49[aa]	221 ± 25[b]	276 ± 67[b]

[a]Different letters indicate significant differences between treatment groups ($p < 0.05$).

Cherry radish seeds were purchased from Hezhiyuan Seed Industry (Shandong Province, China). Snails (*Bradybaena ravida*) were acquired from a breeding facility in Suqian City, Jiangsu Province, China. Following thorough cleaning with ultrapure water, the snails were fed fresh uncontaminated cherry radish shoots and roots for 1 week to acclimate them to the experimental conditions.

Plant Planting and Foliar Spraying with Nanoparticles. The detailed methods for plant culture are provided in Text S2. For the foliar spraying experiment, we estimated the deposition level of DPS (100 μg/d/plant) based on previous studies that investigated the dust retention capacity

https://doi.org/10.1021/acs.est.4c06088
Environ. Sci. Technol. 2024, 58, 21025−21036

and measured mass concentrations of microplastics in dust samples.[43−45] The exposure doses of CeO_2 were set at 100 μg/d/plant, falling within the range of reference NPs application in agriculture and facilitating comparative studies.[46] Specifically, we prepared suspensions of CeO_2, DPS, and a mixture of both at a concentration of 100 mg/L NPs in ultrapure water. Ultrapure water was used as a blank control and all groups were supplemented with 0.1% v/v Tween 20 as a dispersant. Commencing from the 22nd day after transplanting the plants into the soil, a sonicated suspension of NPs (1 mL) was uniformly sprayed onto the leaf surface at 10:00 am daily for a consecutive period of 14 days. This duration coincided with a period of high stomatal conductance in most plants.[47] During foliar exposure, each plant was individually treated on an operating table while ensuring that the shoot, soil, and pot were meticulously covered with aluminum foil and kitchen paper to minimize accidental NP exposure and cross-contamination errors (see Figure S2). Considering the potential loss during the exposure operation, an experiment on spraying efficiency was conducted to determine the actual exposure dose (Text S3, Table S1). A total of four treatment groups were included: control, CeO_2 (100 mg/L in spray solution, equivalent to a dosage of 100 μg/d/plant, an actual exposure dose of 86.3 μg/d/plant), DPS (100 mg/L in spray solution, equivalent to a dosage of 100 μg/d/plant, an actual exposure dose of 81.7 μg/d/plant), and mixture (CeO_2+DPS) (spray solution containing 100 mg/L CeO_2 and 100 mg/L DPS, an actual exposure dose of 83.1 μg CeO_2/d/plant and 80.5 μg DPS/d/plant). Each group had 38 replicates. After 37 days, the plants were harvested. Following gentle cleaning, the shoots and roots were carefully separated before being ultrasonically washed three times with ultrapure water to eliminate surface NPs. Washing experiments have verified the effectiveness of the cleaning procedures (Figure S3, Table S2), which successfully removed most of the adsorbed NPs on the leaf surfaces. The liquid collected from the cleaning procedures was analyzed to determine the ratio of adsorbed and absorbed NPs (Figure S4). The samples were then wiped dry and weighed to record the fresh weight. All samples were divided into two parts: one part was stored at −80 °C for chemical analysis, while the other part was kept at 4 °C for snail feeding.

Feeding Protocol. The snails were fasted for 48 h prior to the experiment in order to ensure consistent consumption at the beginning of exposure. Snails of similar size and weight were selected, and 5 individuals were placed in each transparent glass feeding box as a biological replicate, which was lined with moistened gauze to maintain humidity. The experiment consisted of 8 treatment groups: shoot feeding (control, CeO_2, DPS, mixture) and root feeding (control, CeO_2, DPS, mixture), each with 6 replicates. Feeding plants for each treatment group were uniformly cut into chunks and provided to the snails at a daily intake of 2.5 g of shoots and 3.0 g of roots per box. The gauze was replaced and the boxes were cleaned during each feeding interval to eliminate any potential influence from environmental changes on snail behavior. In addition, unconsumed food and feces were collected daily from the inner walls of the transparent glass feeding boxes for the purpose of calculating ingestion and excretion rates. Further, continuous monitoring of snail weight was carried out. Based on observations from a preliminary study that feeding balance is achieved within 14 days, this fixed feeding pattern was maintained for a duration of 14 days before fasting the snails for an additional period of 48 h in order to obtain postintestinal samples. Subsequently, all snails from each group underwent anesthesia using 75% alcohol after being washed with ultrapure water; they were then quickly dissected into shell, soft tissue, and digestive gland components. All tissues were stored at −80 °C for subsequent analysis.

***In Vitro* Simulation of CeO_2 Dissolution and Release in Plants.** Simulated leaf apoplast fluid, simulated xylem sap, and simulated phloem sap were prepared according to established methods (Table S3) from previous research.[48−50] CeO_2 solutions (50 mg/L) and mixture solutions (50 mg/L CeO_2 and 50 mg/L DPS) were prepared using ultrapure water and these simulated fluids, respectively. The solutions were kept shaking in the dark (100 rpm) throughout the testing period, with 4 mL of liquid sampled at time points of 0, 1, 2, 4, 7, 10, and 14 days. Subsequently, the samples were then filtered (Millipore, 3 kDa, ultrafiltration centrifuge) and acidified with 2% v/v HNO_3 for further detection of dissolved Ce released from CeO_2 NPs.

Chemical Analysis. Following complete freeze-drying, the samples were pulverized using a high through-put tissue grinder (Wonbio-800, Shanghai) and then standardized through an 80-mesh sieve before storage in a constant temperature drying oven for subsequent analysis.

The total concentrations of Ce, Ca, Na, Mg, Al, Cu, Fe, Mg, and Zn in the samples were determined using inductively coupled plasma-mass spectrometry (ICP-MS, iCAPQ, Thermo Fisher Scientific, USA): see Text S4 and Table S4 for details. Single particle inductively coupled plasma mass spectrometry (SP-ICP-MS, NexION2000G, PerkinElmer, CA, USA) analysis was performed on plant samples treated with CeO_2 NPs (information provided in Text S5 and Table S5).

The hydrogen concentration was determined using an elemental analyzer (Elementar Vario EL Cube, Germany). The stable isotope ratio δ^2H was measured with a gas chromatography/elemental analysis/water balance stable isotope mass spectrometer (TRACE 1310/EA Isolink/PreCon/253 Plus IRMS, Thermo Fisher Scientific, USA). See Text S6 for the specific procedure.

During the analysis, one laboratory standard sample was included for calibration of every 10 samples, with each sample tested three times. The long-term standard deviation of the test instrument was $\delta^2H \leq 1.0‰$. The δ values of the USGS 88, USGS 89, USGS 90 and USGS 91 standard samples were linearly fitted with their true values to correct the measured values δ_{sample} further. In line with IUPAC protocols, δ_{sample} is expressed as the per mille difference in atomic ratios of $^2H/^1H$ relative to the Vienna Standard Mean Ocean Water (V-SMOW):

$$AR_{sample} = \left(\frac{\delta_{sample}}{1000} + 1\right) \times AR_{standard} \quad (1)$$

where AR_{sample} and $AR_{standard}$ represent the atomic ratios of $^2H/^1H$ in the samples and standard samples, with $AR_{standard}$ being the constant of 1.56×10^{-4}.

The mass concentration of DPS in the sample was determined as follows:

$$MRD_{sample} = \frac{2 \times AR_{sample}}{2 \times AR_{sample} + 1} \times 100\% \quad (2)$$

https://doi.org/10.1021/acs.est.4c06088
Environ. Sci. Technol. 2024, 58, 21025−21036

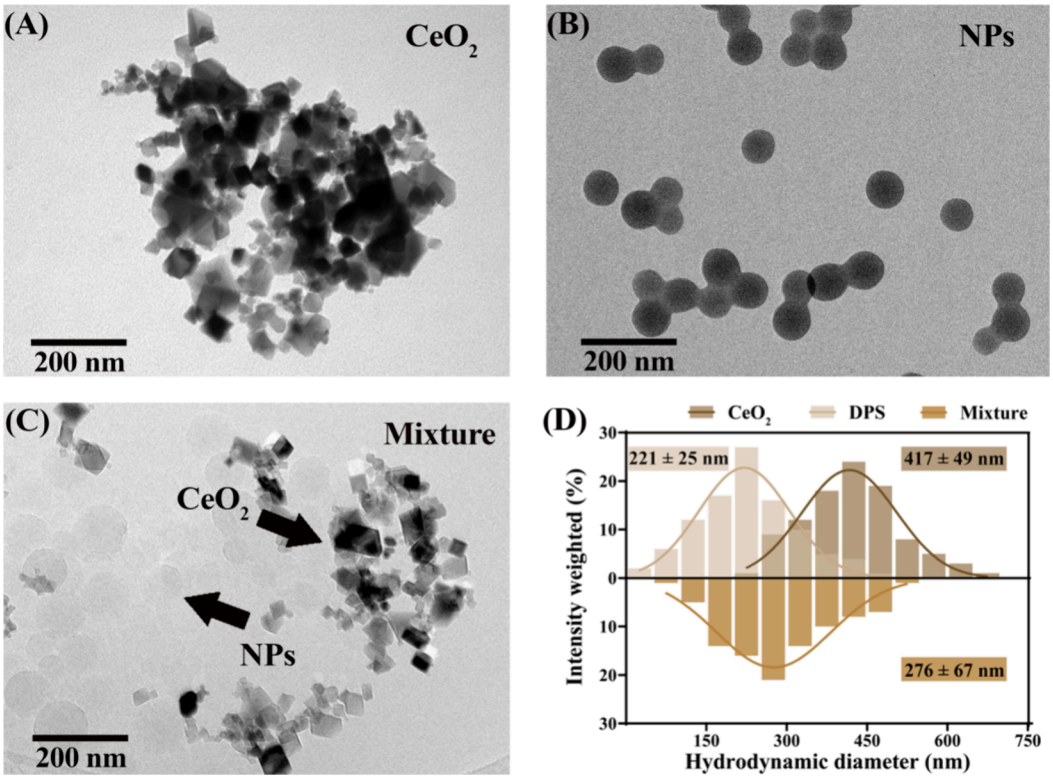

Figure 1. Transmission electron microscopy (TEM) images of nanoparticles (NPs) solution at a concentration of 100 mg/L, including (A) CeO_2 NPs, (B) deuterium-labeled polystyrene (DPS) NPs, and (C) binary NPs mixture. The average hydrodynamic diameters of CeO_2, DPS, and their mixtures are shown in (D).

$$M_{DPS} = \frac{7 \times DW_{sample} \times MRH_{sample} \times (MRD_{sample} - MRD_{control})}{MRD_{DPS}} \quad (3)$$

$$C_{DPS} = \frac{M_{DPS}}{DW_{sample}} = \frac{7 \times MRH_{sample} \times (MRD_{sample} - MRD_{control})}{MRD_{DPS}} \quad (4)$$

where MRD_{sample}, $MRD_{control}$, and MRD_{DPS} denote the mass ratio of deuterium in hydrogen elements in the test sample, control group sample and synthetic DPS, respectively. Meanwhile, MRH_{sample} represents the mass ratio of hydrogen elements in the experimental group sample. The coefficient 7 indicates the ratio of the relative molecular mass of DPS (C_8D_8) to that of deuterium present in DPS. M_{DPS} refers to the total mass of DPS in the sample, DW_{sample} signifies the dry weight of the sample. Consequently, C_{DPS} represents the total mass concentration of deuterium-labeled polystyrene nanoplastics.

Statistics and Analysis. The bioconcentration factor (BCF) and translocation factor (TF) were employed to assess the uptake and transport of NPs by plants, while trophic transfer factors (TTFs), assimilation efficiency (AE), and ingestion rate (IR) were used to quantify the nutrient transfer and animal uptake of nanoparticles. Detailed calculation formulas are provided in Text S7. The mass balance of pollutants in the food chain under the open system was calculated based on the experimentally obtained quantitative data of Ce and DPS in plants and snails (Tables S6 and S7).

Measurement results were presented as mean ± standard deviation (SD). Normality and homogeneity assumptions of data variance were verified, and log transformation was applied when necessary to correct deviations from these assumptions. One-way ANOVA and nonpaired *t*-tests were conducted to determine intergroup differences, with a significance threshold set at 5% ($p < 0.05$). Statistical analysis and graph plotting were performed using GraphPad Prism 8.0.2, Excel 2019, and Origin 2021.

RESULTS AND DISCUSSION

Characterization of Nanoparticles. The TEM images revealed that CeO_2 nanoparticles exhibited a tendency to aggregate, forming irregular agglomerates with an average diameter of 47.8 ± 10.8 nm (n = 50). In contrast, DPS demonstrated superior dispersion as regular spherical particles with an average diameter of 80.7 ± 0.8 nm (n = 50) (Figure 1A,B). Furthermore, the combination of these two particle types resulted in the formation of heterogeneous agglomerates (Figure 1C). The DLS analysis was conducted in ultrapure water at a controlled mass concentration of 100 mg/L CeO_2/DPS and their mixture (CeO_2:100 mg/L, DPS:100 mg/L) (Figure 1D, Table 1). The results showed that the hydrodynamic size of CeO_2 was approximately 417 ± 49 nm, with a zeta potential of −28.4 ± 1.3 mV at pH 5.90. The hydrodynamic size of DPS was 221 ± 25 nm, with a zeta potential of −26.4 ± 1.2 mV at pH 5.96. The hydrodynamic size of nanoparticles in the mixture was 276 ± 67 nm, with a corresponding zeta potential of −28.6 ± 1.1 mV at pH 5.91.

https://doi.org/10.1021/acs.est.4c06088
Environ. Sci. Technol. 2024, 58, 21025−21036

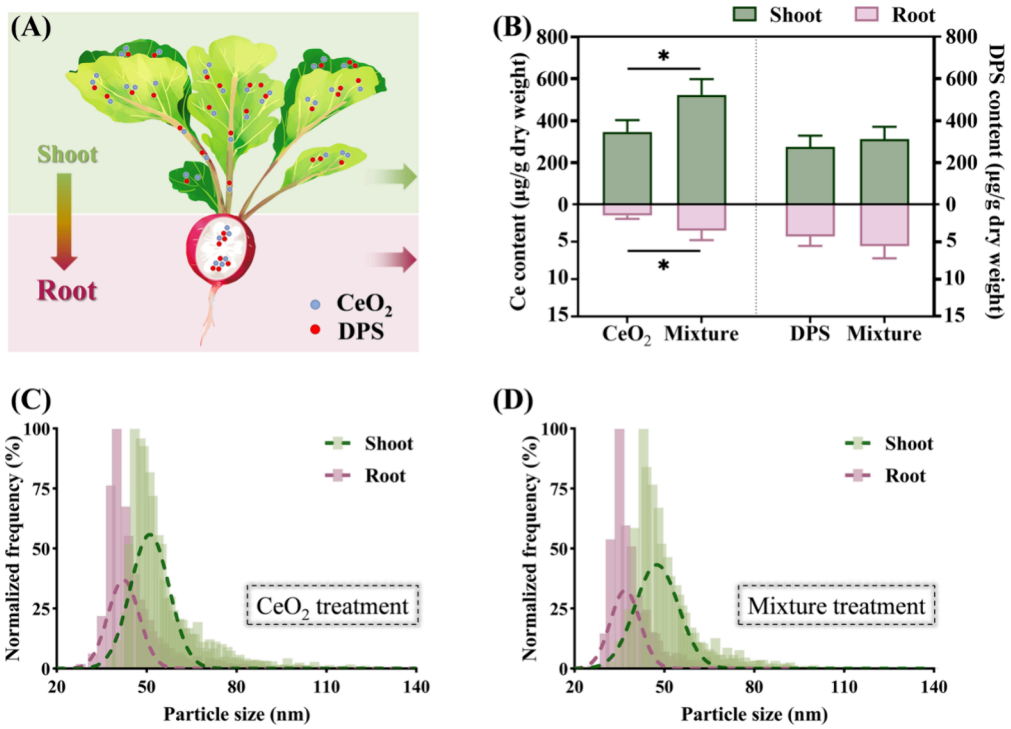

Figure 2. Schematic diagram of the absorption, translocation, and accumulation of CeO_2 and deuterium-labeled polystyrene (DPS) nanoparticles in cherry radish through foliar exposure (A). The contents of Ce and DPS in the shoots and roots of cherry radish upon single and mixture exposures to CeO_2 and DPS nanoparticles (B). Particle size distribution of CeO_2 as measured by SP-ICP-MS in the shoots and roots of cherry radish treated with CeO_2 NPs (C) and mixture NPs (D). The concentration values of all treatment groups have been adjusted by subtracting the background values of the control group (Tables S8 and S9). The data are presented as mean ± SD (n = 6 biological replicates). Significant differences between different groups are denoted as *p < 0.05.

Table 2. Bioconcentration Factor (BCF) of Ce/DPS Transfer from Solution to Plant in Different Treatments, Translocation Factor (TF) of Ce/DPS Transfer from Shoot to Root, Trophic Transfer Factors (TTF) of Ce/DPS Transfer from Shoot/Root to Animal Organs/Total Snail, Assimilation Efficiency (AE) and Ingestion Rate (IR) of Ce/DPS in Shoot-Feeding Snails and Root-Feeding Snails[a]

		Ce transfer			DPS transfer		
		CeO_2	Mixture	p	DPS	Mixture	p
BCF	BCF (solution to plant)	1.42 ± 0.45	2.77 ± 0.14	*	(6.98 ± 1.67) × E-1	(7.33 ± 1.36) × E-1	
TF	TF (shoot to root)	(5.10 ± 0.80) × E-3	(5.20 ± 0.30) × E-3		(2.02 ± 0.28) × E-2	(1.98 ± 0.25) × E-2	
TTF	TTF (shoot to snail)	(3.67 ± 0.30) × E-2	(2.09 ± 0.16) × E-2	*	(4.58 ± 0.42) × E-2	(2.54 ± 0.32) × E-2	*
	TTF (shoot to snail shell)	(1.70 ± 0.50) × E-3	(3.50 ± 0.40) × E-3		(1.80 ± 0.40) × E-3	(8.00 ± 2.00) × E-4	*
	TTF (shoot to snail soft tissues)	(4.90 ± 1.30) × E-3	(6.20 ± 1.50) × E-3		(4.95 ± 0.96) × E-2	(2.06 ± 0.45) × E-2	*
	TTF (shoot to digestive gland)	(1.32 ± 0.46) × E-2	(8.46 ± 3.22) × E-2	*	(4.89 ± 0.52) × E-2	(1.31 ± 0.18) × E-1	
	TTF (shoot to snail feces)	8.18 ± 0.54	5.59 ± 0.28	*	6.68 ± 0.47	11.1 ± 1.5	*
	TTF (root to snail)	(8.20 ± 1.25) × E-1	(3.32 ± 0.67) × E-1	*	(5.51 ± 0.88) × E-1	(6.13 ± 0.97) × E-1	
	TTF (root to snail shell)	(3.91 ± 0.61) × E-1	(3.19 ± 0.49) × E-1		(1.62 ± 0.39) × E-2	(2.93 ± 0.20) × E-2	*
	TTF (root to snail soft tissues)	(2.26 ± 0.41) × E-1	(1.36 ± 0.04) × E-1	*	(5.78 ± 0.80) × E-1	1.01 ± 0.23	*
	TTF (root to digestive gland)	(7.10 ± 1.70) × E-1	(2.23 ± 0.41) × E-1	*	(7.16 ± 1.96) × E-1	1.32 ± 0.18	*
	TTF (root to snail feces)	4.79 ± 0.67	1.93 ± 0.21	*	3.31 ± 0.10	2.63 ± 0.18	*
AE (%)	AE (shoot feeding snails)	2.50 ± 0.52	3.95 ± 0.66	*	11.1 ± 4.9	1.81 ± 0.78	*
	AE (root feeding snails)	76.5 ± 3.2	70.1 ± 12.3		65.5 ± 16.5	76.2 ± 13.4	
IR (g/g/d)	IR (shoot feeding snails)	(3.68 ± 0.71) × E-2	(4.84 ± 1.25) × E-2		(5.72 ± 0.47) × E-2	(9.86 ± 2.03) × E-2	*
	IR (root feeding snails)	(1.01 ± 0.17) × E-1	(4.17 ± 1.44) × E-2	*	(1.73 ± 0.20) × E-1	(7.33 ± 1.01) × E-2	*

[a]Values are expressed as mean ± SD (n = 6). Different letters and "*" indicates a significant difference between treatment groups in the same parameter (p < 0.05).

Accumulation and Translocation of Ce and DPS in Plants. The 14-day foliar exposure of CeO_2, DPS, and their mixtures resulted in the absorption of Ce or DPS via the plant leaves (Figure 2). In radish shoots, significantly higher concentrations of Ce were observed after the mixture treatment (522 ± 70 μg/g) compared to that found in single CeO_2 treatment (365 ± 42 μg/g) (p < 0.05). This difference in the calculated whole-plant BCF for Ce was consistently observed, with values of 1.42 ± 0.46 and 2.77 ± 0.14 after single CeO_2 treatment and mixture treatment, respectively (p <

https://doi.org/10.1021/acs.est.4c06088
Environ. Sci. Technol. 2024, 58, 21025−21036

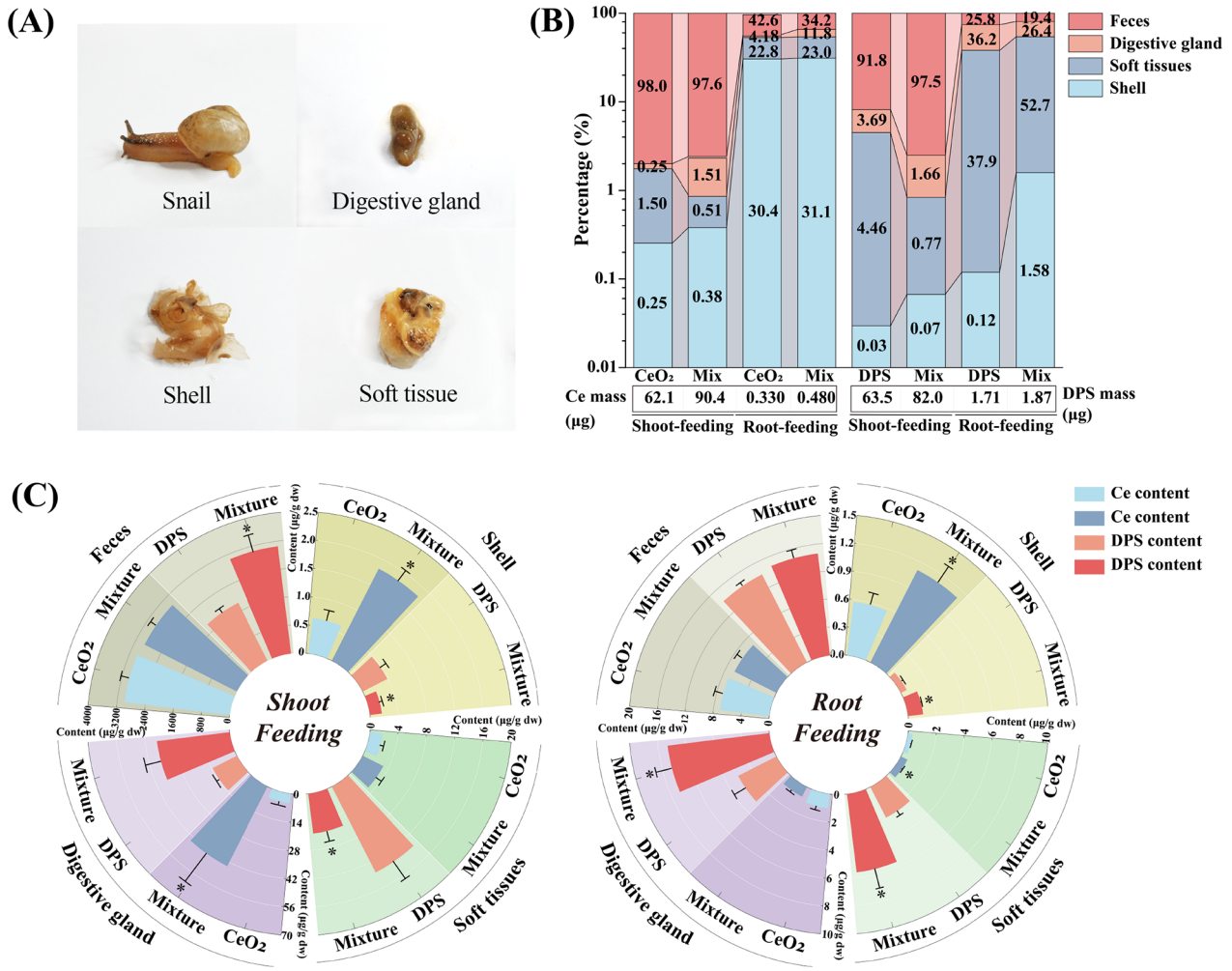

Figure 3. Experimental photographs illustrating the dissection of a snail into three parts: shell, soft tissues, and digestive gland (A). Total mass ratio (B) and concentrations (C) of Ce and deuterium-labeled polystyrene (DPS) in the three body parts and feces of shoot-feeding snails and root-feeding snails. (B) The mass percentage figures of the pollutant are indicated in each bar, with the total mass displayed at the bottom of each column. The concentration values of all treatment groups have been adjusted by subtracting the background values of the control group (Tables S8 and S9). The data are presented as mean ± SD (n = 6 experimental parallel samples). Significant differences between different groups are denoted as *p < 0.05.

0.05) (Table 2). These results show that foliar uptake of Ce is promoted by the presence of DPS.

A comparison between single DPS treatment and mixture treatment revealed that the concentrations of DPS in radish shoots were 275 ± 49 μg/g and 311 ± 54 μg/g, respectively. The BCF values for DPS in the entire plants were determined to be 0.70 ± 0.17 and 0.73 ± 0.14 under the two treatments. The presence of CeO_2 did not significantly alter the uptake of DPS by plants.

The inconsistent effects of mixture exposure on the leaf surface uptake of Ce and DPS can be attributed to changes in the properties of NPs resulting from aggregation. These effects are influenced by hydrophobicity, $\pi-\pi$ stacking, and electrostatic interactions between particles.[51] In the CeO_2-DPS mixture solution, there was no significant change in zeta potential compared to either the single CeO_2 or single DPS dispersions, while the hydrodynamic diameter was significantly smaller than that of the single CeO_2 solution (p < 0.05) and similar to the hydrodynamic diameter of the single DPS suspension (Figure 1D, Table 1). The charge and size of test NPs are considered key factors limiting leaf uptake. The cell wall and cuticle of plants typically carry negative charges with a higher affinity for positive charges, as demonstrated by Wang et al., where positively charged PS (PS-NH^{3+}) accumulated more in lettuce leaves than negatively charged PS (PS-COO^{-}).[43] The biological barrier imposed by leaves restricts particle of specific particle size, as observed by Li et al., where smaller-sized ZnO NPs accumulated more in the cytoplasm of rice seedlings. This caused more severe cell damage, while larger-sized NPs were effectively blocked.[52] Therefore, it is reasonable to speculate that changes in aggregate size in this study could lead to differences in leaf uptake.

Foliar uptake followed by Ce or DPS translocated from aboveground to underground parts (Figure 2). In radish roots, Ce concentration in single CeO_2 treatment (1.47 ± 0.38 μg/g) were significantly lower than that in mixture treatment (3.48 ± 1.17 μg/g) (p < 0.05), while the TF remained similar at around 5.10 × 10^{-3} for both treatments (Table 2). In single DPS and mixture treatments, the respective contents were 4.26 ± 1.15 μg/g and 5.56 ± 1.48 μg/g and the respective TF values were calculated as 2.02 × 10^{-2} and 1.98 × 10^{-2}. Indeed, mixture treatments do not affect transport capability of plants for Ce or DPS. In addition, a significant disparity in the translocation factor of Ce and DPS in plants was observed,

https://doi.org/10.1021/acs.est.4c06088
Environ. Sci. Technol. 2024, 58, 21025−21036

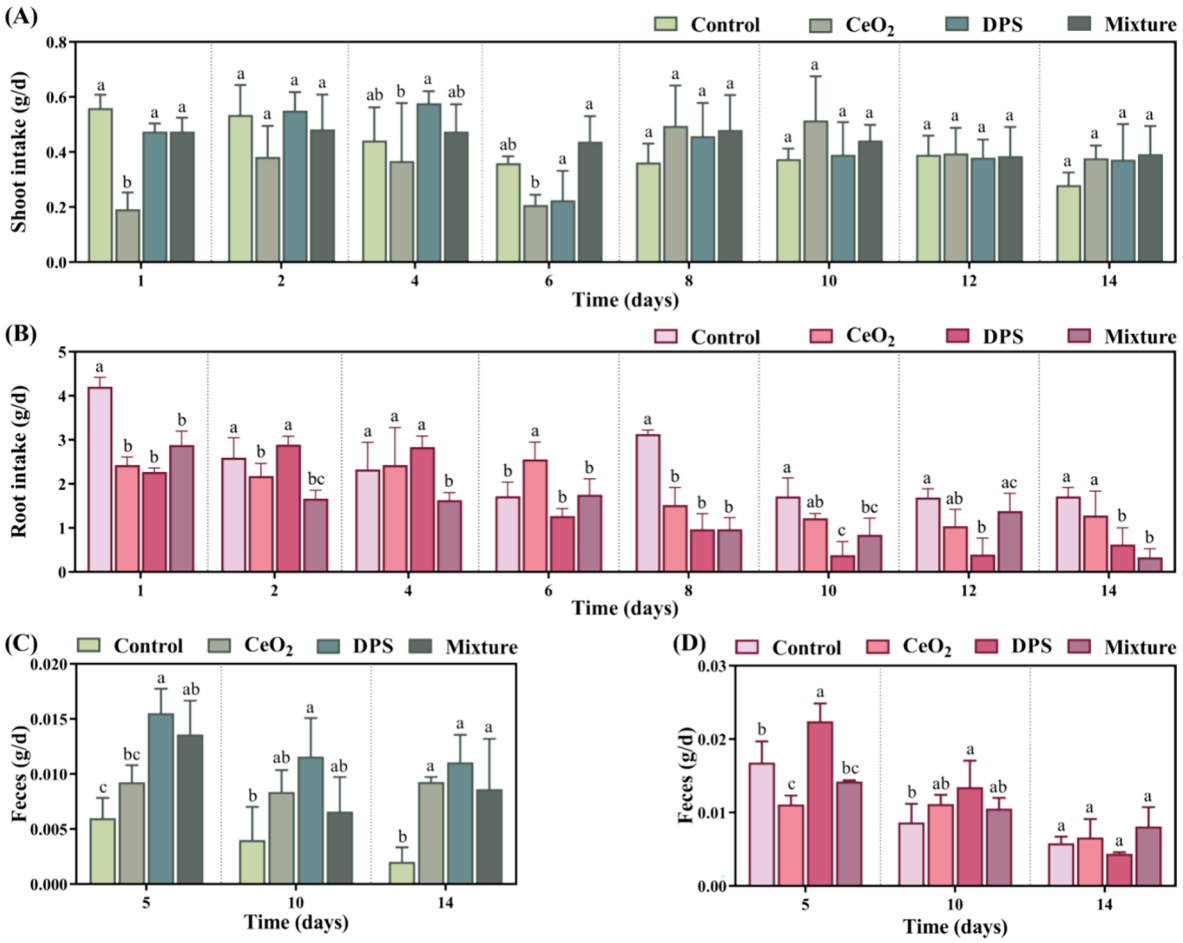

Figure 4. Changes in food intake fresh weight of shoot-feeding snails (A) and root-feeding snails (B), and dry weight fecal excretion of shoot-feeding snails (C) and root-feeding snails (D) during the feeding period. Each column represents the daily average during the observation period. The data are presented as mean ± SD (n = 6 replicate samples). Different letters indicate significant differences between treatment groups in the same observation cycle ($p < 0.05$).

irrespective of single or mixture treatment, indicating that DPS exhibits higher ease of translocation in cherry radish. *In situ* observations conducted on tomatoes and wheat revealed deformation and compression of internalized polystyrene NPs within intercellular spaces.[44,53] This morphological change suggests the importance of the material properties of the NPs in their interaction with plant cell structures. Considering the Young's modulus of CeO_2 (207−228 GPa) and DPS (2.1 GPa), it can be speculated a low mechanical strength of NPs may facilitate their translocation within plants.[41] The reduced resistance to deformation allows DPS to navigate through plant tissues more easily, enhancing their movement from shoot to root. This could have important implications for understanding how various NPs behave within plant systems and their potential ecological impacts.

Trophic Transfer of Ce and DPS. Nanoparticles could enter and accumulate in various parts of snails through the food chain. To quantify the NPs, we analyzed dissected snails and their feces (Figure 3A). Results revealed accumulation of Ce and DPS in all treatments (Figure 3C). Within the shoot-snail food chain, the mixture treatment exhibited elevated concentrations of Ce in both the shell and digestive glands compared to the single treatment. In contrast, DPS levels were higher in feces and lower in shell and soft tissues under the mixture treatment. In the root-snail food chain, the mixture treatment showed increased Ce concentrations in the shell and soft tissues compared to the single treatment. In addition, DPS concentrations were significantly higher in the shell, soft tissues and digestive glands following mixture treatment. The observed patterns suggest a synergistic accumulation of Ce in snails consuming plants contaminated with mixed NPs in both shoot and root pathways.

Overall, the TTF values for Ce and DPS showed a significant decline in the total shoot-feeding snails following mixture treatments compared to single treatments to NPs. The TTF values for Ce in shoot-feeding snails (single exposure: 3.67×10^{-2}, mixture exposure: 2.09×10^{-2}) were found to be similar to those observed in a previous study involving a lettuce-snail food chain (TTF value: 3.70×10^{-2}).[23] In contrast, for root-feeding snails as a whole, the TTF value for Ce significantly decreased following mixture treatments compared to single treatments, while there was no significant difference in the TTF value for DPS after mixture treatments. Additionally, regardless of the single or mixed exposure to CeO_2 or DPS, the TTF value from root to the total snail was an order of magnitude higher than the TTF value from the shoots to the total snail. The trophic transfer of Ce and DPS was specifically driven by the type of food source.

Comparing the TTFs of Ce or DPS in different organismal parts, the effects of mixture exposure on various parts did not

https://doi.org/10.1021/acs.est.4c06088
Environ. Sci. Technol. 2024, 58, 21025−21036

show consistent effects with the overall effects on snails as previously discussed (Table 2). For instance, in shoot-feeding snails, the TTF values for Ce in the shell and soft tissues were not different in the mixture treatment compared to the single CeO_2 treatment, while the TTF value for Ce in the digestive gland was higher. However, at the organism level, TTF values for Ce were lower in the mixture treatment. In root-feeding snails, the TTF values for DPS in shell, soft tissue and digestive gland were higher in the mixture treatment compared to the single DPS treatment, but there was no difference in the overall TTF value for DPS in snails. This discrepancy can be attributed to the dynamic processes of pollutant absorption, distribution, metabolism, and elimination within different tissues or organs, leading to varied accumulation patterns. In all treatments, TTF values for Ce or DPS in feces were 1−2 orders of magnitude higher than TTF values in other parts of the snails, indicating that snails could excrete CeO_2 and DPS captured through consuming plants. This finding is consistent with previous studies on CeO_2 along the pakchoi-snail and polystyrene along lettuce-snail food chains.[22] Particularly, TTF values greater than 1 were exclusively observed in the digestive gland (1.01 ± 0.23) and soft tissues (1.32 ± 0.18) of snails that consumed radish roots exposed to mixtures, indicating a trophic transfer-mediated biomagnification of DPS originating from NPs changing during translocation and mixed NPs interaction. In this study, a 14-day exposure duration was adopted assuming that pollutants reach an absorption-excretion equilibrium in biota. Future studies should consider prolonged exposure periods to adequately assess and predict the ecological risks associated with the long-term trophic transfer of target pollutants through food chains.

In summary, compared to single treatments, mixture treatments pronouncedly affected the trophic transfer of Ce and DPS. However, the transfer may be promoted or inhibited depending on the food chain and the type of nanomaterials involved. Moreover, the influence of exposure to mixtures may not be consistent across both the overall and local aspects of consumers. Conversely, previous studies constructing a lettuce-snail food chain found that exposure of lettuce to nano-Ag or nano-TiO_2 or their mixture did not affect the trophic transfer of Ag or Ti.[21] These conflicting results can be attributed to various factors including species variations, NPs type, size and concentration, and environmental influences.

In general, NPs are thermodynamically unstable due to their high surface area to volume ratio. In this study, CeO_2 and DPS may have interacted with each other and have undergone complex physical and chemical transformation processes, such as dissolution, adsorption, chelation, aggregation, and dispersion, thereby affecting their further environmental behaviors. For example, previous research has demonstrated that when subjected to mixture treatments with nano-TiO_2 and nano-ZnO, the adsorption of Zn^{2+} onto nano TiO_2 weakened the inhibitory effect of nano-ZnO on bacterial ATP levels.[54] Additionally, it has also been reported that nano-CeO_2 and nano-ZnO mixtures displayed higher cytotoxicity to *Nitrosomonas europaea* compared to single NPs due to enhanced synergistic effect mediated by electrostatic interactions between these distinct NPs and cells.[55] These interactions play a crucial role in determining the behavior of NPs mixtures within organisms. However, their effects may vary depending on the specific materials involved since metal oxide NPs generally exhibit greater environmental activity than other types of NPs.[52] This variability could potentially explain the observed fluctuations in trophic transfer efficiency associated with NPs mixture exposures as observed in our study. In addition to microlevel interactions between CeO_2 NPs and DPS NPs, mixture treatments may also disrupt trophic transfer efficiency by altering the behavior of snails. While no changes in snail body weight were observed in any treatment, differences in ingestion and excretion rates between the single CeO_2 or DPS treatments and mixture treatments were noted (Figure S5, Figure 4). The presence of NPs mixture could potentially affect the palatability of plant-based foods, resulting in a direct negative impact on consumer feeding behavior. The inhibition of consumer feeding behavior may stem from the toxicity of NPs resulting from trophic transfer. It has been reported that snails consumed green beans contaminated with PS NPs experienced a reduction in food intake, which was associated with a decline in gut microbiota viability and histological damage in the digestive organs due to NP accumulation.[56] This underscores the ecological toxicity of NPs, indicating their potential to disrupt not only individual species but also broader food chain interactions. Additionally, the NPs mixture may also influence plants, indirectly altering consumer behavior by modulating plant metabolism.[57] Previous research has shown that silicon quantum dots can enhance the physical resistance of radishes to whitefly larvae by increasing the accumulation of silicon and lignin, as well as boosting chemical defense mechanisms against root-feeding insects through the upregulation of secondary metabolites such as jasmonic acid, salicylic acid, and diterpenes.[58] In our study, the different interference of CeO_2, DPS, or their mixture on the mineral element homeostasis in cherry radish shoots and roots (Figure S6) were indicative of activation of plant metabolic defenses. This activation may impact snail behavior, as various elements play essential roles in plant metabolism by providing energy and serving as enzyme components.[59,60] However, further evidence from metabolite data is needed to support this hypothesis.

Biodistribution of NPs in Snails. The distribution of pollutants in snails, as indicated by the proportion of localized mass to their total mass, exhibited a distinct pattern depending on whether the snails consume shoots or roots as their dietary source (Figure 3B). Specifically, the distribution of Ce in shoot-feeding snails showed a ranking pattern of feces (98.0%) > soft tissues (1.50%) > digestive glands (0.25%) = shell (0.25%) in single treatment, while in mixture treatment, the ranking pattern shifted to feces (97.6%) > digestive glands (1.51%) > soft tissues (0.51%) > shell (0.38%). The distribution of DPS in shoot-feeding snails remained similar to Ce in both single treatments and mixture treatments. Snails consuming shoots adjusted their distribution strategy of Ce and DPS when exposed to a mixture of CeO_2 and DPS NPs, with more Ce and DPS entering the snail digestive glands rather than the soft tissues.

In root-feeding snails, the distribution of Ce in both single treatment and mixture treatment maintained the same ranking of feces (CeO_2 treatment: 42.6%, mixture treatment: 34.2%) > shell (CeO_2 treatment: 30.4%, mixture treatment: 31.1%) > soft tissues (CeO_2 treatment: 22.8%, mixture treatment: 23.0%) > digestive glands (CeO_2 treatment: 4.18%, mixture treatment: 11.8%). The internal distribution of DPS NPs remained unchanged in cases of single or mixture treatments, with a ranking of soft tissues (DPS treatment: 39.7%, mixture treatment: 52.7%) > digestive glands (DPS treatment: 36.2%, mixture treatment: 26.4%) > feces (DPS treatment: 25.8%,

https://doi.org/10.1021/acs.est.4c06088
Environ. Sci. Technol. 2024, 58, 21025−21036

mixture treatment: 19.4%) > shell (DPS treatment: 0.12%, mixture treatment: 1.58%). The distribution pattern of root-feeding snails remained unaltered when exposed to a mixture of CeO_2 and DPS NPs compared to single exposure. However, a significant difference was observed in the biodistribution mode of Ce and DPS in root-feeding snails. In contrast to Ce, DPS was found to be more likely to remain in the snail's body rather than being eliminated through the feces.

Combining the overall distribution patterns of Ce and DPS in snails with the assimilation rate (AE) (Figure 3B, Table 2), it is evident that the mixture treatments boosted the AE value for Ce while diminishing the AE value for DPS in shoot-feeding snails. The mixture treatments had no effect on AE value for Ce or DPS in root-feeding snails. Importantly, in both single and mixture treatments, the bioavailability of Ce and DPS for root-feeding snails was significantly higher than the bioavailability observed in shoot-feeding snails, revealing an order-of-magnitude difference in AE values. Correspondingly, from shoot-feeding snails to root-feeding snails, the percentage for Ce decreased from 97.6−98.0% to 34.2−42.6%, and the percentage for DPS decreased from 91.8−97.5% to 19.4−25.8%. This underscores a consistent trend: the bioavailability of NPs significantly increases following their translocation from shoots to roots. Several factors may contribute to the observed variances in bioavailability. First, differences in the morphological properties of NPs in shoots and roots may influence their bioavailability. Analysis using SP-ICP-MS has revealed that the average size of CeO_2 NPs in shoots (CeO_2 treatment: 59.3 ± 0.3 nm, mixture treatment: 54.2 ± 1.0 nm) is larger than that of CeO_2 NPs in roots (CeO_2 treatment: 48.4 ± 1.8 nm, mixture treatment: 41.3 ± 0.2 nm) (Figure 2C,D). During leaf absorption and translocation, size exclusion limits may prevent larger individual NPs or aggregates from reaching the roots. Nanoparticles dispersed in radish roots may depend on smaller sizes with a higher probability of being transferred into the snail's body rather than being excreted. Furthermore, *in vitro* tracking simulations indicated that the dissolution of CeO_2 NPs and the release of Ce ions occur in simulated xylem sap (Figure S7). These results are consistent with previous research,[61,62] suggesting that CeO_2 in NP form within leaves may undergo partial dissolution during transport or after reaching the roots. Although there is currently a lack of experimental evidence on the changes of DPS in plants, such transformations during the translocation process appear to be essential for the bioavailability of NPs. Second, food texture can significantly influence the bioavailability of NPs. Compared to cherry radish shoots, taproots containing indigestible lignified fibers result in longer residence times in the gastrointestinal tract of snails. This prolonged residence time may contribute to a greater release of NPs into the digestive system of the snails.[63] Moreover, certain reducing metabolites stored in plant roots, as well as specific metabolic antioxidant compounds synthesized by plants, such as reducing sugars, flavonoids, and ascorbic acid, may play crucial roles in triggering redox reactions during the biotransformation of NPs that enhance their absorption and utilization by snails.[64,65] Lastly, when NPs enter plants, they selectively adsorb surrounding biomolecules from the complex physiological fluid environment. This process results in the formation of coronas composed of proteins, lipids, sugars, nucleic acids, and natural organic compounds. This biocorona grants NPs "biological properties" distinct from their "synthetic properties", subsequently affecting cellular internalization, distribution, and accumulation of NPs in organisms.[66−68]

Environmental Implications. This study presented the first quantitative analysis of the accumulation, trophic transfer, and biodistribution of CeO_2, DPS, and their mixture along the cherry radish-snail food chain. In the context of increasing airborne nanoplastic pollution and burgeoning nanotechnology in agriculture, our investigation identified foliar exposure as a crucial pathway for NPs to be transferred through the food chain. This study demonstrated inconsistent effects of mixed NPs exposure patterns on the uptake and distribution of Ce and DPS in cherry radishes and snails. Further exploration is warranted to comprehend the mechanisms driving NPs trophic transfer, particularly in mixture exposure scenarios. Moreover, although the accumulated amount of NPs decreased after being transported to plant roots, it significantly altered their biological distribution pattern at higher trophic levels, resulting in a higher accumulation of NPs within organisms rather than excretion through feces. The observed biomagnification, changes in snail behavior, and disturbances in the elemental balance of plant and animal highlight the necessity for more comprehensive studies to understand the ecological risks associated with trophic transfer of NPs.

■ ASSOCIATED CONTENT

Supporting Information

The Supporting Information is available free of charge at https://pubs.acs.org/doi/10.1021/acs.est.4c06088.

Deuterated polystyrene synthesis methods, plant culture methods, ICP-MS analysis methods and operation parameters, isotope analysis methods, calculation formula for bioconcentration factor, translocation factor, trophic transfer factors (TTF), assimilation efficiency (AE), and ingestion rate (IR), FTIR and TEM images of deuterated polystyrene, experimental photographs, biomass and element content of plants, body weight of snails, and biomass and element content of snails (PDF)

■ AUTHOR INFORMATION

Corresponding Author

Hao Qiu − *School of Environmental Science and Engineering, Shanghai Jiao Tong University, Shanghai 200240, China;* orcid.org/0000-0002-4743-9702; Email: haoqiu@sjtu.edu.cn

Authors

Yingxin Chen − *School of Environmental Science and Engineering, Shanghai Jiao Tong University, Shanghai 200240, China*

Erkai He − *School of Geographic Sciences, East China Normal University, Shanghai 200241, China;* orcid.org/0000-0002-4866-3001

Willie J.G.M. Peijnenburg − *Center for the Safety of Substances and Products, National Institute of Public Health and the Environment, Bilthoven 3720 BA, The Netherlands; Institute of Environmental Sciences, Leiden University, Leiden 2300 RA, The Netherlands;* orcid.org/0000-0003-2958-9149

Xiaofeng Jiang − *School of Environmental Science and Engineering, Shanghai Jiao Tong University, Shanghai 200240, China*

Complete contact information is available at:

https://doi.org/10.1021/acs.est.4c06088
Environ. Sci. Technol. 2024, 58, 21025−21036

https://pubs.acs.org/10.1021/acs.est.4c06088

Notes

The authors declare no competing financial interest.

■ ACKNOWLEDGMENTS

This study was financially supported by the National Key Research and Development Program of China (no. 2023YFC3711500) and the National Natural Science Foundation of China (no. 42377268).

■ REFERENCES

(1) Samrot, A. V.; Ram Singh, S. P.; Deenadhayalan, R.; Rajesh, V. V.; Padmanaban, S.; Radhakrishnan, K. Nanoparticles, a double-edged sword with oxidant as well as antioxidant properties—a review. *Oxygen* **2022**, *2* (4), 591−604.
(2) Harrison, D. M.; Briffa, S. M.; Mazzonello, A.; Valsami-Jones, E. A review of the aquatic environmental transformations of engineered nanomaterials. *Nanomaterials* **2023**, *13* (14), 2098.
(3) Zhao, X.; Sun, J.; Zhou, L.; Teng, M.; Zhao, L.; Li, Y.; Wu, F. Defining the size ranges of polystyrene nanoplastics according to their ability to cross biological barriers. *Environmental Science: Nano* **2023**, *10* (10), 2634−2645.
(4) Plastics Europe*Plastic-the Facts*; 2022, https://plasticseurope.org/knowledge-hub/plastics-the-facts-2022/, accessed 2024−08−26.
(5) Gigault, J.; El Hadri, H.; Nguyen, B.; Grassl, B.; Rowenczyk, L.; Tufenkji, N.; Feng, S.; Wiesner, M. Nanoplastics are neither microplastics nor engineered nanoparticles. *Nat. Nanotechnol.* **2021**, *16* (5), 501−507.
(6) Elsakhawy, T. A.; Omara, A. E.-D.; Amer, M. M.; El-Ramady, H. R.; Prokisch, J.; Brevik, E. A diagrammatic mini review on soil human health nexus: with focus on soil nano pollution. *Environment, Biodiversity and Soil Security* **2022**, *6* (2022), 327−338.
(7) Jan, N.; Majeed, N.; Ahmad, M.; Lone, W. A.; John, R. Nano-pollution: Why it should worry us. *Chemosphere* **2022**, *302*, No. 134746.
(8) Zhao, X.; Yu, M.; Xu, D.; Liu, A.; Hou, X.; Hao, F.; Long, Y.; Zhou, Q.; Jiang, G. Distribution, bioaccumulation, trophic transfer, and influences of CeO_2 nanoparticles in a constructed aquatic food web. *Environ. Sci. Technol.* **2017**, *51* (9), 5205−5214.
(9) Dang, F.; Huang, Y.; Wang, Y.; Zhou, D.; Xing, B. Transfer and toxicity of silver nanoparticles in the food chain. *Environmental Science: Nano* **2021**, *8* (6), 1519−1535.
(10) Zahra, Z.; Habib, Z.; Hyun, S.; Sajid, M. Nanowaste: another future waste, its sources, release mechanism, and removal strategies in the environment. *Sustainability* **2022**, *14* (4), 2041.
(11) Hong, J.; Wang, L.; Sun, Y.; Zhao, L.; Niu, G.; Tan, W.; Rico, C. M.; Peralta-Videa, J. R.; Gardea-Torresdey, J. Foliar applied nanoscale and microscale CeO_2 and CuO alter cucumber (*Cucumis sativus*) fruit quality. *Sci. Total Environ.* **2016**, *563*, 904−911.
(12) Schreck, E.; Foucault, Y.; Sarret, G.; Sobanska, S.; Cécillon, L.; Castrec-Rouelle, M.; Uzu, G.; Dumat, C. Metal and metalloid foliar uptake by various plant species exposed to atmospheric industrial fallout: mechanisms involved for lead. *Sci. Total Environ.* **2012**, *427*, 253−262.
(13) Larue, C.; Castillo-Michel, H.; Sobanska, S.; Cécillon, L.; Bureau, S.; Barthès, V.; Ouerdane, L.; Carrière, M.; Sarret, G. Foliar exposure of the crop *Lactuca sativa* to silver nanoparticles: evidence for internalization and changes in Ag speciation. *Journal of Hazardous Materials* **2014**, *264*, 98−106.
(14) Burkhardt, J.; Basi, S.; Pariyar, S.; Hunsche, M. Stomatal penetration by aqueous solutions-an update involving leaf surface particles. *New Phytologist* **2012**, *196* (3), 774−787.
(15) Avellan, A.; Yun, J.; Morais, B. P.; Clement, E. T.; Rodrigues, S. M.; Lowry, G. Critical review: Role of inorganic nanoparticle properties on their foliar uptake and in planta translocation. *Environ. Sci. Technol.* **2021**, *55* (20), 13417−13431.
(16) De la Rosa, G.; Vázquez-Núñez, E.; Molina-Guerrero, C.; Serafín-Muñoz, A. H.; Vera-Reyes, I. Interactions of nanomaterials and plants at the cellular level: current knowledge and relevant gaps. *Nanotechnol. Environ. Eng.* **2021**, *6*, 7.
(17) Eichert, T.; Kurtz, A.; Steiner, U.; Goldbach, H. Size exclusion limits and lateral heterogeneity of the stomatal foliar uptake pathway for aqueous solutes and water-suspended nanoparticles. *Physiologia plantarum* **2008**, *134* (1), 151−160.
(18) Larue, C.; Castillo-Michel, H.; Sobanska, S.; Trcera, N.; Sorieul, S.; Cécillon, L.; Ouerdane, L.; Legros, S.; Sarret, G. Fate of pristine TiO_2 nanoparticles and aged paint-containing TiO_2 nanoparticles in lettuce crop after foliar exposure. *Journal of Hazardous Materials* **2014**, *273*, 17−26.
(19) Chichiriccò, G.; Poma, A. Penetration and toxicity of nanomaterials in higher plants. *Nanomaterials* **2015**, *5* (2), 851−873.
(20) Wang, W.-N.; Tarafdar, J. C.; Biswas, P. Nanoparticle synthesis and delivery by an aerosol route for watermelon plant foliar uptake. *J. Nanopart. Res.* **2013**, *15*, 1417.
(21) Wu, J.; Bosker, T.; Vijver, M. G.; Peijnenburg, W. J. Trophic transfer and toxicity of (mixtures of) Ag and TiO_2 nanoparticles in the lettuce−terrestrial snail food chain. *Environ. Sci. Technol.* **2021**, *55* (24), 16563−16572.
(22) Wang, Y.; Ma, C.; Dang, F.; Zhao, L.; Zhou, D.; Gu, X. Mixed effects and co-transfer of CeO_2 NPs and arsenic in the pakchoi-snail food chain. *Journal of Hazardous Materials* **2024**, *462*, No. 132770.
(23) Ma, Y.; Yao, Y.; Yang, J.; He, X.; Ding, Y.; Zhang, P.; Zhang, J.; Wang, G.; Xie, C.; Luo, W.; Zhang, J.; Zheng, L.; Chai, Z.; Zhao, Y.; Zhang, Z. Trophic transfer and transformation of CeO_2 nanoparticles along a terrestrial food chain: influence of exposure routes. *Environ. Sci. Technol.* **2018**, *52* (14), 7921−7927.
(24) Guo, J.; Liu, N.; Xie, Q.; Zhu, L.; Ge, F. Polystyrene microplastics facilitate the biotoxicity and biomagnification of ZnO nanoparticles in the food chain from algae to daphnia. *Environ. Pollut.* **2023**, *324*, No. 121181.
(25) Maharramov, A. M.; Hasanova, U. A.; Suleymanova, I. A.; Osmanova, G. E.; Hajiyeva, N. E. The engineered nanoparticles in food chain: Potential toxicity and effects. *SN Appl. Sci.* **2019**, *1*, 1362.
(26) Wu, J.; Sun, J.; Bosker, T.; Vijver, M. G.; Peijnenburg, W. J. Toxicokinetics and particle number-based trophic transfer of a metallic nanoparticle mixture in a terrestrial food chain. *Environ. Sci. Technol.* **2023**, *57* (7), 2792−2803.
(27) Judy, J. D.; Unrine, J. M.; Bertsch, P. M. Evidence for biomagnification of gold nanoparticles within a terrestrial food chain. *Environ. Sci. Technol.* **2011**, *45* (2), 776−781.
(28) Dai, Y.; Wang, Z.; Zhang, L.; Jiang, Z.; Pu, S.; Fan, Q.; Zhao, J.; Xing, B. Transfer and transformation of CeO_2 NPs along a terrestrial trophic food chain. *Environmental Science: Nano* **2020**, *7* (2), 588−598.
(29) Petersen, E. J.; Barrios, A. C.; Henry, T. B.; Johnson, M. E.; Koelmans, A. A.; Montoro Bustos, A. R.; Matheson, J.; Roesslein, M.; Zhao, J.; Xing, B. Potential artifacts and control experiments in toxicity tests of nanoplastic and microplastic particles. *Environ. Sci. Technol.* **2022**, *56* (22), 15192−15206.
(30) Li, Z.; Li, R.; Li, Q.; Zhou, J.; Wang, G. Physiological response of cucumber (*Cucumis sativus* L.) leaves to polystyrene nanoplastics pollution. *Chemosphere* **2020**, *255*, No. 127041.
(31) Wang, K.; Wang, Y.; Li, K.; Wan, Y.; Wang, Q.; Zhuang, Z.; Guo, Y.; Li, H. Uptake, translocation and biotransformation of selenium nanoparticles in rice seedlings (*Oryza sativa* L.). *J. Nanobiotechnol.* **2020**, *18* (1), 103.
(32) Ma, Y.; Zhang, P.; Zhang, Z.; He, X.; Zhang, J.; Ding, Y.; Zhang, J.; Zheng, L.; Guo, Z.; Zhang, L.; Chai, Z.; Zhao, Y. Where does the transformation of precipitated ceria nanoparticles in hydroponic plants take place? *Environ. Sci. Technol.* **2015**, *49* (17), 10667−10674.
(33) Auobi Amirabad, S.; Behtash, F.; Vafaee, Y. Selenium mitigates cadmium toxicity by preventing oxidative stress and enhancing photosynthesis and micronutrient availability on radish (*Raphanus*

sativus L.) cv. Cherry Belle. *Environmental Science and Pollution Research* **2020**, *27* (11), 12476−12490.
(34) Wu, Y.; Ta, H. T. Different approaches to synthesising cerium oxide nanoparticles and their corresponding physical characteristics, and ROS scavenging and anti-inflammatory capabilities. *J. Mater. Chem. B* **2021**, *9* (36), 7291−7301.
(35) Zeng, Q.; Yu, C.; Chang, X.; Wan, Y.; Ba, Y.; Li, C.; Lv, H.; Guo, Z.; Cai, T.; Ren, Z.; Qin, Y.; Zhang, Y.; Ma, K.; Li, J.; He, S.; Wan, H. CeO_2 nanohybrid as a synergist for insecticide resistance management. *Chem. Eng. J.* **2022**, *446*, No. 137074.
(36) Allen, S.; Allen, D.; Phoenix, V. R.; Le Roux, G.; Durántez Jiménez, P.; Simonneau, A.; Binet, S.; Galop, D. Atmospheric transport and deposition of microplastics in a remote mountain catchment. *Nature Geoscience* **2019**, *12* (5), 339−344.
(37) Evangeliou, N.; Grythe, H.; Klimont, Z.; Heyes, C.; Eckhardt, S.; Lopez-Aparicio, S.; Stohl, A. Atmospheric transport is a major pathway of microplastics to remote regions. *Nat. Commun.* **2020**, *11* (1), 3381.
(38) Sheng, X.; Lai, Y.; Yu, S.; Li, Q.; Zhou, Q.; Liu, J. Quantitation of atmospheric suspended polystyrene nanoplastics by active sampling prior to pyrolysis−gas chromatography−mass spectrometry. *Environ. Sci. Technol.* **2023**, *57* (29), 10754−10762.
(39) Liu, K.; Wang, X.; Song, Z.; Wei, N.; Li, D. Terrestrial plants as a potential temporary sink of atmospheric microplastics during transport. *Sci. Total Environ.* **2020**, *742*, No. 140523.
(40) Cai, G.; Xu, S.; Wang, Z.; Wilkie, C. A. Further studies on polystyrene/cerium (IV) oxide system: melt blending and interaction with montmorillonite. *Polym. Adv. Technol.* **2014**, *25* (2), 217−222.
(41) Bani-Salameh, A. A.; Ahmad, A.; Alsaad, A.; Qattan, I.; Aljarrah, I. A. Synthesis, optical, chemical and thermal characterizations of PMMA-PS/CeO_2 nanoparticles thin film. *Polymers* **2021**, *13* (7), 1158.
(42) Tian, L.; Chen, Q.; Jiang, W.; Wang, L.; Xie, H.; Kalogerakis, N.; Ma, Y.; Ji, R. A carbon-14 radiotracer-based study on the phototransformation of polystyrene nanoplastics in water versus in air. *Environmental Science: Nano* **2019**, *6* (9), 2907−2917.
(43) Wang, Y.; Xiang, L.; Wang, F.; Wang, Z.; Bian, Y.; Gu, C.; Wen, X.; Kengara, F. O.; Schäffer, A.; Jiang, X.; Xing, B. Positively charged microplastics induce strong lettuce stress responses from physiological, transcriptomic, and metabolomic perspectives. *Environ. Sci. Technol.* **2022**, *56* (23), 16907−16918.
(44) Shi, R.; Liu, W.; Lian, Y.; Wang, X.; Men, S.; Zeb, A.; Wang, Q.; Wang, J.; Li, J.; Zheng, Z.; Zhou, Q.; Tang, J.; Sun, Y.; Wang, F.; Xing, B. Toxicity mechanisms of nanoplastics on crop growth, interference of phyllosphere microbes, and evidence for foliar penetration and translocation. *Environ. Sci. Technol.* **2024**, *58* (2), 1010−1021.
(45) Jia, M.; Zhou, D.; Lu, S.; Yu, J. Assessment of foliar dust particle retention and toxic metal accumulation ability of fifteen roadside tree species: Relationship and mechanism. *Atmospheric Pollution Research* **2021**, *12* (1), 36−45.
(46) Zhang, H.; Lu, L.; Zhao, X.; Zhao, S.; Gu, X.; Du, W.; Wei, H.; Ji, R.; Zhao, L. Metabolomics reveals the "invisible" responses of spinach plants exposed to CeO_2 nanoparticles. *Environ. Sci. Technol.* **2019**, *53* (10), 6007−6017.
(47) De Oliveira, J. P. V.; Duarte, V. P.; De Castro, E. M.; Magalhães, P. C.; Pereira, F. J. Stomatal cavity modulates the gas exchange of *Sorghum bicolor* (L.) Moench. grown under different water levels. *Protoplasma* **2021**, *259*, 1081−1097.
(48) Zhang, Y.; Fu, L.; Li, S.; Yan, J.; Sun, M.; Giraldo, J. P.; Matyjaszewski, K.; Tilton, R. D.; Lowry, G. V. Star polymer size, charge content, and hydrophobicity affect their leaf uptake and translocation in plants. *Environ. Sci. Technol.* **2021**, *55* (15), 10758−10768.
(49) Gao, X.; Kundu, A.; Bueno, V.; Rahim, A. A.; Ghoshal, S. Uptake and translocation of mesoporous SiO_2-coated ZnO nanoparticles to *Solanum lycopersicum* following foliar application. *Environ. Sci. Technol.* **2021**, *55* (20), 13551−13560.
(50) Rodrigues, S.; Avellan, A.; Bland, G. D.; Miranda, M. C.; Larue, C.; Wagner, M.; Moreno-Bayona, D. A.; Castillo-Michel, H.; Lowry, G. V.; Rodrigues, S. M. Effect of a zinc phosphate shell on the uptake and translocation of foliarly applied ZnO nanoparticles in pepper plants (*Capsicum annuum*). *Environ. Sci. Technol.* **2024**, *58* (7), 3213−3223.
(51) Cai, X.; Liu, X.; Jiang, J.; Gao, M.; Wang, W.; Zheng, H.; Xu, S.; Li, R. Molecular mechanisms, characterization methods, and utilities of nanoparticle biotransformation in nanosafety assessments. *Small* **2020**, *16* (36), No. 1907663.
(52) Gong, D.; Bai, X.; Weng, Y.; Kang, M.; Huang, Y.; Li, F.; Chen, Y. Phytotoxicity of binary nanoparticles and humic acid on *Lactuca sativa L. Environmental Science: Processes Impacts* **2022**, *24* (4), 586−597.
(53) Li, L.; Luo, Y.; Li, R.; Zhou, Q.; Peijnenburg, W. J.; Yin, N.; Yang, J.; Tu, C.; Zhang, Y. Effective uptake of submicrometre plastics by crop plants via a crack-entry mode. *Nature Sustainability* **2020**, *3* (11), 929−937.
(54) Tong, T.; Wilke, C. M.; Wu, J.; Binh, C. T. T.; Kelly, J. J.; Gaillard, J.-F. o.; Gray, K. A. Combined toxicity of nano-ZnO and nano-TiO_2: from single-to multinanomaterial systems. *Environ. Sci. Technol.* **2015**, *49* (13), 8113−8123.
(55) Zhao, L.; Sun, Y.; Hernandez-Viezcas, J. A.; Hong, J.; Majumdar, S.; Niu, G.; Duarte-Gardea, M.; Peralta-Videa, J. R.; Gardea-Torresdey, J. L. Monitoring the environmental effects of CeO_2 and ZnO nanoparticles through the life cycle of corn (*Zea mays*) plants and in situ μ-XRF mapping of nutrients in kernels. *Environ. Sci. Technol.* **2015**, *49* (5), 2921−2928.
(56) Chae, Y.; An, Y.-J. Nanoplastic ingestion induces behavioral disorders in terrestrial snails: trophic transfer effects via vascular plants. *Environmental Science: Nano* **2020**, *7* (3), 975−983.
(57) Hatami, M.; Kariman, K.; Ghorbanpour, M. Engineered nanomaterial-mediated changes in the metabolism of terrestrial plants. *Sci. Total Environ.* **2016**, *571*, 275−291.
(58) Fan, N.; Zhao, C.; Chang, Z.; Yue, L.; He, F.; Xiao, Z.; Wang, Z. J. E. S. N. Silicon quantum dots promote radish resistance to root herbivores without impairing rhizosphere microenvironment health. *Environmental Science: Nano* **2023**, *10* (9), 2232−2244.
(59) Kaur, H.; Kaur, H.; Kaur, H.; Srivastava, S. J. P. G. R. The beneficial roles of trace and ultratrace elements in plants. *Plant Growth Regulation* **2023**, *100* (2), 219−236.
(60) Aguirre-Becerra, H.; Vazquez-Hernandez, M. C.; Saenz de la O, D.; Alvarado-Mariana, A.; Guevara-Gonzalez, R. G.; Garcia-Trejo, J. F.; Feregrino-Perez, A. A. Role of stress and defense in plant secondary metabolites production. *Bioactive Natural Products for Pharmaceutical Applications* **2021**, *140*, 151−195.
(61) Hayder, M.; Wojcieszek, J.; Asztemborska, M.; Zhou, Y.; Ruzik, L. Analysis of cerium oxide and copper oxide nanoparticles bioaccessibility from radish using SP-ICP-MS. *Journal of the Science of Food Agriculture* **2020**, *100* (13), 4950−4958.
(62) Wang, J.; Yue, L.; Zhao, J.; Cao, X.; Wang, C.; Chen, F.; Xiao, Z.; Feng, Y.; Wang, Z. Uptake and bioaccumulation of nanoparticles by five higher plants using single-particle-inductively coupled plasma-mass spectrometry. *Environmental Science: Nano* **2022**, *9* (8), 3066−3080.
(63) Schäfer, J.; Brett, A.; Trierweiler, B.; Bunzel, M. Characterization of cell wall composition of radish (*Raphanus sativus* L. var. *sativus*) and maturation related changes. *J. Agric. Food Chem.* **2016**, *64* (45), 8625−8632.
(64) Beattie, I. R.; Haverkamp, R. G. Silver and gold nanoparticles in plants: sites for the reduction to metal. *Metallomics* **2011**, *3* (6), 628−632.
(65) Hassan, A. D.; Abdul-ameer, M. A. Effect of plant metabolism on some qualitative characteristics of root exudates among different plants. *Dijlah J. Agric. Sci.* **2023**, *1* (2), 44−53.
(66) Abdolahpur Monikh, F.; Chupani, L.; Arenas-Lago, D.; Guo, Z.; Zhang, P.; Darbha, G. K.; Valsami-Jones, E.; Lynch, I.; Vijver, M. G.; van Bodegom, P. M.; Peijnenburg, W. J. G. M. Particle number-based trophic transfer of gold nanomaterials in an aquatic food chain. *Nat. Commun.* **2021**, *12*, 899.

(67) Wang, C.; Chen, B.; He, M.; Hu, B. Composition of intracellular protein corona around nanoparticles during internalization. *ACS Nano* **2021**, *15* (2), 3108−3122.
(68) Li, L.; Li, S.; Xu, Y.; Ren, L.; Yang, L.; Liu, X.; Dai, Y.; Zhao, J.; Yue, T. Distinguishing the nanoplastic−cell membrane interface by polymer type and aging properties: translocation, transformation and perturbation. *Environmental Science: Nano* **2023**, *10* (2), 440−453.

https://doi.org/10.1021/acs.est.4c06088
Environ. Sci. Technol. 2024, 58, 21025−21036